NATIONAL ADVISORY COMMITTEE FOR AERONAUTICS

TECHNICAL NOTE 3996

INVESTIGATION OF A SHORT-ANNULAR-DIFFUSER CONFIGURATION UTILIZING SUCTION AS A MEANS OF BOUNDARY-LAYER CONTROL

By Stafford W. Wilbur and James T. Higginbotham

Langley Aeronautical Laboratory
Langley Field, Va.

Washington

June 1957

NATIONAL ADVISORY COMMITTEE FOR AERONAUTICS

TECHNICAL NOTE 3996

INVESTIGATION OF A SHORT-ANNULAR-DIFFUSER CONFIGURATION UTILIZING SUCTION AS A MEANS OF BOUNDARY-LAYER CONTROL

By Stafford W. Wilbur and James T. Higginbotham

SUMMARY

A straight outer-wall annular diffuser having a center-body length of one-half the outer-body diameter and an area ratio of 1.9:1 has been investigated for mean inlet flow angles of 0° and 19.5° in order to determine the effect of area suction applied on the inner wall. The entrance shape, number, and location of the openings through which the air was removed were varied. The auxiliary air flow was varied from 0 to approximately 4 percent of the main stream air flow; the mean inlet Mach number was approximately 0.26.

For most of the configurations, significant improvement in performance was obtained over no control when a suction flow rate of as little as 1 percent was utilized. Increased rates of suction were responsible for some additional improvements depending on the configuration of suction openings. Rounding the entrance of the suction holes and increasing the area through which suction was applied effectively decreased the auxiliary flow losses and thereby produced higher values of diffuser effectiveness. The diffuser-exit velocity distributions were also improved by the increase in suction area and by an increase in the amount of suction.

INTRODUCTION

The general purpose of this investigation was to develop a short diffuser design that is applicable to turbojet-engine installations. Specifically, the objective was to achieve a minimum total-pressure loss and a uniform exit velocity distribution within a diffuser length of 1.0 outer-body diameter or less. Previous research has indicated that this objective can be accomplished only through the use of boundary-layer controls.

The effects of vortex generators in diffusers with center-body lengths varying from zero to 1.0 outer-body diameters are reported in references 1 to 5. Suction and injection control by means of slots on very short diffusers is described in references 6 and 7. From a study of the results of the investigations of references 1 to 5, it was evident that the most favorable velocity distributions were obtained at the downstream station corresponding to a length-diameter ratio of 1.0 when the center-body length was 50 to 60 percent of the outer-body diameter. In addition, references 6 and 7 indicated that designs with good aerodynamic shapes should be used in conjunction with suction control in order to reduce to a minimum the auxiliary flow quantities and pumping requirements. Whirling flow at the diffuser inlet also must be removed by straighteners (see ref. 2) before efficient diffusion can be accomplished in the type of design under study.

The present investigation employs suction from an appreciable surface area of the center body in contrast with suction from a discrete slot as in reference 7. The center-body configuration is about the same length as the longer configuration of reference 7, its length being 50 percent of the outer-body diameter. The effect of whirling flow at the inlet, with and without a flow-straightener installation, was investigated because of the possible application as a turbine discharge diffuser in which appreciable whirl exists under some operating conditions. The investigation was conducted with fully developed pipe flow at the inlet of the diffuser, which had a 21-inch constant outer-wall diameter and an area ratio of 1.9:1. The mean inlet Mach number was maintained nearly constant at 0.26 with a corresponding Reynolds number, based on inlet hydraulic diameter, of 1.6×10^6. The mean angles of flow at the inlet were 0° and 19.5°.

SYMBOLS

D	diameter
p	static pressure
p_t	total pressure
Δp	static-pressure rise
Δp_t	total-pressure loss

q_c	compressible impact pressure, $p_t - p$
u	local velocity within boundary layer
y	radial distance from the diffuser outer wall
M	Mach number
w	mass flow
R	ratio of auxiliary air mass flow to main-stream mass flow, percent
N_R	Reynolds number based on the inlet hydraulic diameter
C_P	pumping-power coefficient
η	diffuser effectiveness
θ	flow angle

Subscripts:

1	diffuser inlet station
1a	reference static pressure station
2,3	diffuser tailpipe stations
x	diffuser station
t	total velocity of whirling flow
A	axial component of total velocity

A bar over a symbol indicates a weighted average.

APPARATUS AND PROCEDURE

General Apparatus

The main air flow was sucked through the general test apparatus (fig. 1(a)) by a fan. The air entered an inlet bell that was covered with a fine mesh cloth. Before entering the diffusing region and downstream duct, the air passed through an annular-approach duct which was approximately 27 feet long and which had a constant inner diameter

of $14\frac{1}{2}$ inches and an outer diameter that varied from 21 to 25 inches. The center body was used for the auxiliary air duct and contained an orifice designed according to the specifications of reference 8. For the whirling-flow tests, a set of fixed guide vanes was installed just downstream of the inlet bell to give a whirling motion to the main-stream air flow. The resulting weighted mean flow angle at the diffuser inlet was 19.5°.

Diffuser Model

The diffuser center body shown in figures 1(b) and 1(c) was very nearly elliptical in the profile cross section and had a length that corresponds to a 31° equivalent cone angle. The shape was identical to that of configuration 3 of reference 5 in order to obtain comparable results. Rows of suction holes were drilled normal to the center-body surface at center-body diameters of 13.08, 12.54, 11.88, 11.14, and 10.24 inches for rows 1 to 5, respectively. Each row contained eighteen $\frac{3}{8}$-inch equispaced holes, indexed $6\frac{2}{3}°$ around the circumference from those of the previous row. The holes were tested with both square and rounded leading edges.

For part of the whirling-flow tests, flow-straightener vanes were mounted on the outer wall 2 inches downstream from the inlet station (measured from the 30-percent-chord point) at an angle of attack of 0°. These flow straighteners were symmetrical rectangular NACA 0012 airfoils with 3-inch chords and 3-inch spans. Twenty-four were equispaced around the outer-wall periphery.

Instrumentation

A single row of static-pressure orifices was installed longitudinally along the diffuser outer wall from the diffuser inlet station to a point approximately 3 diameters downstream. Four equispaced static-pressure orifices on the diffuser outer wall were installed at stations 1, 1(a), and 3. Surveys of stagnation and static pressures and flow angle were made at stations 1, 2, and 3 by using two probes spaced 180° apart at each station. Two shielded reference total-pressure tubes were installed permanently 180° apart in the center of the annular passage upstream from the diffuser inlet. A shielded total-pressure tube was also installed inside the center body to measure the recovery of the suction air.

Test Procedure

The investigation was initiated by obtaining pressure measurements for axial flow with no suction holes (no suction boundary-layer control).

After these measurements were obtained, the origin of the separated-flow region was determined by visual observations of small wool tufts attached to the center body and was found to coincide with the row of suction holes labeled row 2 (see fig. 1(b)). This row of suction holes was drilled and performance measurements were taken with varying suction rate. The holes were then rounded on the outer edge to reduce the suction power required. Successive rows of holes were drilled, the edges were rounded, and tests were made in order to determine the effect of varying the number of rows and of their position. A mixture of oil and lampblack was used to study the flow along the center body when rows 1, 2, and 3 were used for suction of approximately 2 percent. When this method was used to observe the flow, thin bands of oil and lampblack were painted at critical locations on the center body to clarify the flow phenomena in the vicinity of the suction holes and immediately downstream of this region.

After the axial-flow tests, the whirling-flow tests with varying rates of suction through rows 2, 3, and 4 were initiated. Data were taken with and without the flow straighteners installed.

Bases for Comparison of Results

The velocity distributions across the duct at stations 1, 2, and 3 are presented in terms of $u/\bar{u}_1$, a ratio of the local velocity to the average velocity of the fully developed pipe flow at the diffuser inlet. The angular distribution across the duct θ is presented with the velocity distribution for the whirling-flow inlet condition. The longitudinal static-pressure distribution along the outer wall is presented in terms of $\frac{\Delta p_{x-1a}}{\bar{q}_{c,1}}$, a ratio of the difference in the local wall static pressure and the wall static pressure at station 1a to the mass-weighted compressible impact pressure at station 1. For axial flow, the static-pressure rise between stations 1 and 3 obtained with various amounts of auxiliary flow is presented in terms of $\frac{\overline{\Delta p}_{3-1}}{\bar{q}_{c,1}}$, which is similar to the term used in presenting the longitudinal distribution except that four circumferentially spaced orifices are used to obtain mean static pressures at stations 1 and 3. For the whirling-flow inlet condition, the static-pressure rise is presented in terms of $\frac{\overline{\Delta p}_{3-1}}{\bar{q}_{c,1}}$, a ratio of the difference between mass-weighted static pressures at stations 1 and 3 to the mass-weighted total compressible impact pressure at station 1.

In the presentation of the diffuser performance, pumping power chargeable to the auxiliary air flow has been incorporated into the

results. The pumping-power coefficient C_P, as described in reference 6, assumes that the pump is 100-percent efficient and that the pump should increase the total-pressure level of the suction air to that of station 1. The pumping-power coefficient is given by the following formula:

$$C_P = \frac{R}{100} \frac{\bar{p}_{t,1} - p_{t,\text{suction}}}{\bar{q}_{c,1}}$$

The resulting diffuser effectiveness is then

$$\eta = \frac{\Delta p_{\text{actual}}}{\Delta p_{\text{ideal}}}$$

$$= \frac{\left(\frac{\Delta p_{3-1}}{\bar{q}_{c,1}}\right)_{\text{actual}}}{\left(\frac{\Delta p_{3-1}}{\bar{q}_{c,1}}\right)_{\text{ideal}} + C_P}$$

The ideal static-pressure-rise coefficient for axial inlet flow is defined as the isentropic one-dimensional pressure rise based on the area ratio and the mass-weighted impact pressure at station 1. For whirling flow at the inlet with flow straighteners installed, the ideal static-pressure rise was obtained in the same manner by assuming that the flow straighteners removed all the whirl with no losses. For whirling flow with no flow straighteners, no satisfactory definition of diffuser effectiveness was determined since for vortex flow the whirl component of the inlet flow theoretically would become infinite on the diffuser center line at the exit. Thus, the static-pressure rise would become negative infinity.

The diffuser loss coefficient is defined as $\frac{\overline{\Delta p_{t,1-3}}}{\bar{q}_{c,1}} + C_P$. This coefficient is subject to measurement errors because of the difficulties in measuring total pressure in a velocity gradient with high turbulence. Measurement errors of this type are discussed in reference 7. A downstream station where total pressure could have been measured accurately was not available in the setup.

In order to obtain an idea of the magnitude of the measurement error, surveys at station 3 were integrated to obtain the mass flow; the results were compared with integrated mass-flow measurements at the diffuser inlet, which should be accurate. These results are presented in figure 2 and indicate that for axial flow the mass-flow discrepancies vary from about 6 percent to 19 percent, the variation depending on the suction configuration and the amount of suction flow. Suction reduced the mass-flow

discrepancies by producing more uniform velocity distributions and by reducing the turbulence level near the inner wall. Test conditions with higher discrepancies, such as were encountered with axial inlet flow, are more optimistic with regard to the loss coefficient.

With whirling flow and no flow straighteners, the mass-flow discrepancies were of the order of 2 percent, which is evidence of the ability of rotation to suppress turbulence. With whirling flow and straightener vanes, the mass-flow discrepancy was again comparable with that obtained with axial inlet flow.

For comparative purposes, the loss coefficient as presented should be sufficiently accurate.

RESULTS AND DISCUSSION

Inlet Flow Conditions

The inlet flow conditions are a necessary factor for obtaining the performance of a diffuser. In addition to the importance of the boundary layer at the inlet as an influence on the subsequent diffusion process, the pressure measurements obtained at this station are used in the determination of the overall diffuser performance coefficients. Inlet velocity distributions for the axial-flow and whirling-flow conditions are presented in figure 3. The boundary layer, similar to fully developed pipe flow, filled the entire annulus, and the use of flow controls had no effect on the inlet conditions for the range of variables tested. For axial flow the velocity profile was nearly symmetrical about the annulus center line. For whirling flow, total, axial, and rotational components of velocity are given in terms of the mean value of each. These profiles are unsymmetrical, the maximum velocity occurring near the outer wall. The axial component is similar to the total velocity profile because of the small flow-angle variation.

Visual-Flow Observations With Axial Flow

Flow observations for axial flow, with 2-percent suction through rows 1, 2, and 3 (fig. 4), were carried out by using rings of oil and lampblack in the positions indicated. The patterns obtained indicated almost equal flow through each hole and localized regions of relatively high-velocity flow downstream from each hole in row 3. Suction through a porous material would probably have resulted in more uniform flow downstream of the suction area. At a distance of $2\frac{1}{2}$ inches downstream from row 3, there was no evidence of flow except for two small regions

of reverse flow. This region (about 14 percent of the exit area) would be reduced in size by use of higher suction rates or suction holes downstream from row 3.

Performance With Axial Flow

Velocity distributions.- The velocity distributions at stations 2 and 3 are presented in figures 5 to 8 for the various combinations of suction rows investigated.

Figure 5 is presented for comparative purposes to show the velocity distributions obtained with suction through row 2 with either sharp-edge or rounded holes. With no holes and therefore no control, approximately a 3-inch-diameter core of reverse flow was indicated at station 2. The distribution was considerably improved at station 3 because of the natural mixing in the intervening duct length. Rounding the sharp edge of the suction holes had no apparent effect on the velocity distributions. With suction solely through row 2, an increase in the suction rate from 1 percent to about 2 percent had a small adverse effect at station 3.

For the remaining combinations of suction-hole rows (figs. 6 to 8), increasing suction produced improved velocity distributions near the central region of the duct and caused higher velocity deficiencies near the outer wall. The latter result is due to the increased diffuser pressure rise causing deterioration of the boundary layer on the outer wall. This condition indicates that control on the outer wall is also needed. One-percent suction was frequently not sufficient to eliminate the evidence of reverse flow at station 2.

The effects of varying the number of rows of holes or their location are shown in figures 9(a) and 9(b) for suction flow rates of about 2.3 percent and 3.4 percent, respectively. The profiles show that increasing the number of rows or shifting the suction area downstream produced improvements in the velocity distribution near the central region. More improvement in the distributions was evident with $R \approx 2.3$ percent than with $R \approx 3.4$ percent.

Longitudinal static-pressure distributions.- The longitudinal wall static-pressure distributions for the various combinations of suction rows are presented in figure 10. For suction flow rates of 2.3 percent and 3.4 percent, the number of rows of holes, location of rows, or configuration of holes had little or no effect on the measured static-pressure rise along the outer wall. A suction flow rate of 2.3 percent produced increases in the static-pressure-rise coefficient of 60 percent and 25 percent at stations 2 and 3, respectively. For one of the best suction-hole configurations, correcting for the suction pumping power

reduced the 25-percent increase in static-pressure rise at station 3 to 22.6 percent. A suction flow rate of about 1 percent frequently was not sufficient to control separation, especially for the cases in which four rows of holes were used. This result possibly may be due to flow recirculation through the holes. Therefore, for this amount of suction, the number of rows used did have an effect on the static-pressure-rise coefficient.

Performance coefficients.- The pumping-power coefficient is presented in figure 11; from this figure the primary variable is seen to be the total hole area. Rounding the sharp edge decreased the pumping power by 30 percent. A small advantage resulted by shifting the rows downstream toward the high-pressure end of the diffuser.

The ideal pumping-power-coefficient curve represents the lower limit which would be approached if the total hole area were increased to very large values. The curve was calculated on the assumption that in the limiting case the suction total-pressure recovery would equal the inner-wall static pressure at the suction-hole location. Inasmuch as the inner-wall static pressures were not measured, the outer-wall pressures were used in the calculation. Use of these outer-wall pressures resulted in low values of pumping power. The curve shows that, for the cases with four rows of holes and a suction flow rate of 3 percent, approximately 40 percent of the pumping power was due to the losses through the holes and 60 percent was due to pressure deficiencies of the suction flow before it entered the openings. Therefore, additional savings in pumping power could have been obtained by using a larger total hole area.

The static-pressure coefficient at station 3 is presented in figure 12, and, as previously noted, neither the number of rows nor the configuration of holes had any appreciable effect on the static-pressure rise except for the lower rates of suction through rows 2, 3, 4, and 5. Figure 12 indicates an optimum suction flow rate of about 2.8 percent. The rapid deterioration of the outer-wall boundary layer at the higher values of suction causes the static-pressure coefficient to decrease for $R > 2.8$ percent and indicates that boundary-layer control is needed on the outer wall also. (See ref. 1.)

When the measured static-pressure-rise coefficient is put in terms of diffuser effectiveness and corrected for pumping power, the optimum suction quantity varies with the number of rows of holes because of the variation of pumping power with total hole area. A maximum diffuser effectiveness of 81.5 percent is indicated for the configurations with three and four rows of holes. (See fig. 12.) If the pumping-power coefficient were reduced to a minimum by enlarging the holes, a maximum effectiveness of 83.5 percent would be obtained for a suction rate of 2.8 percent. Further gains in effectiveness would have to be obtained by control on the outer wall.

For flow rates in excess of 1 percent, the measured loss coefficient (fig. 12) was not affected by the number of rows of suction holes used and showed a continuous reduction with an increase in the suction flow rate. Correction for pumping power produces an optimum suction flow rate for each hole configuration in a manner similar to the diffuser effectiveness. Even when the loss coefficient is corrected for pumping power, the resulting values are lower than that obtained for no control over most of the range of suction quantities for each configuration. For one of the best suction-hole configurations, a suction flow rate of 2.3 percent decreased the measured total-pressure loss by 63 percent; correcting for the suction pumping power reduced the 63-percent reduction to 30 percent.

Performance With Whirling Flow

Velocity and flow-angle distributions.- The ratio of the radial distribution of the local total velocity to the mean inlet total velocity is presented in figure 13 along with the flow-angle distribution across the duct at stations 2 and 3 for the diffuser without flow straighteners. The flow angles were reduced by suction control in the region $5 < y < 8$ at both stations. In the remaining duct regions, the flow angles were increased by control. The most severe increase occurred on the duct center line where reverse flow was indicated ($\theta > 90°$). Suction on the diffuser inner wall inherently increases the flow angle near the duct center line because of the law of conservation of angular momentum.

The velocity distributions were improved by suction in the region 5 to 9 inches from the outer wall at station 2. The effect of suction was to produce less uniform total-velocity distributions at station 3 and to establish reverse flow near the duct center line.

With rotation, with or without suction, the axial-flow component of whirling flow at stations 2 and 3 was more uniform than the axial inlet flow condition except in the region near the duct center line (fig. 14). Suction with whirling flow improved the axial-velocity component over most of the duct area; however, it also intensified the reverse flow near the center line.

Rotation had some favorable influence on the diffusion process; however, considerable energy is represented in the rotational component at stations 2 and 3 and would have to be recovered to make the process efficient. Rotation could possibly be used to advantage in some configurations in which the amount and distribution of rotation was controlled.

The effect of flow straighteners in conjunction with whirling flow is illustrated in figure 15. The flow angles at station 2 were reduced by the flow straighteners from the outer wall to a distance of 4 inches from the outer wall; however, the straighteners were less effective over

the remaining duct area because of the 1/4-inch gap that existed between the inner wall and the tips of the straightening vanes and, also, because of the very low axial velocities in this region. The flow angles at station 3 were more uniformly low with the straighteners because of the increased uniformity of the axial component. The velocity distributions at stations 2 and 3 were nonuniform with or without suction.

Performance coefficients.- The static-pressure-rise coefficient between stations 1 and 3 is presented in figure 16; low values are indicated with no flow straighteners with or without suction because of the high flow angles (mean flow angle of about 41°). Without flow straighteners, suction increased the static-pressure rise by only a slight amount. This result is the net effect of a reduction in loss due to the fact that suction is almost counteracted by an increase in the flow angle. With flow straighteners, suction increased the static-pressure rise an appreciable amount. This result is principally due to the large reduction in loss caused by suction.

The diffuser effectiveness η with straightener vanes (fig. 16) did not increase as rapidly as the static-pressure-rise coefficient because of the pumping-power correction. The effectiveness was much lower than that for the axial inlet flow condition with or without suction because of the losses through the vanes, because of the lack of effectiveness of suction in improving the velocity distribution, and, also, because of the unrecovered energy represented by the rotation.

The mean flow angle (fig. 16) doubled between the inlet and exit stations without flow straighteners. Flow straighteners were responsible for a reduction in the mean flow angle of about 30° at the exit stations; however, for good performance the flow angle should have been reduced even more. Suction, in general, was responsible for an increase in the flow angle.

The loss coefficient for whirling flow with and without straightener vanes is presented in figure 16. Whirl reduced the measured loss coefficient about 30 percent without suction but the use of flow straighteners doubled the value obtained without flow straighteners. Part of this increase is believed to be due to the increased diffuser losses with the straighteners. The measured-loss curves indicate much less reduction in loss produced with suction without straighteners than with straighteners. This result shows that, with high flow angles and no flow straighteners, the total-pressure deficiencies along the inner wall are very small because of the more favorable pressure gradient. The loss coefficient corrected for pumping power produces optimum suction quantities of about 1 percent. This low value is caused by the relatively high pumping-power coefficient as compared to the improvements obtained through suction.

SUMMARY OF RESULTS

The performance of an annular diffuser with a constant-diameter outer wall and a center body the length of which was equal to one-half the outer-body diameter was determined for inlet conditions corresponding to a fully developed boundary layer: a Mach number of 0.26, a Reynolds number of 1.6×10^6, and mean flow angles of 0° and 19.5°. The diffuser area ratio was 1.9:1. Suction through discrete holes was used to control the inner-wall boundary layer.

Axial Flow

The results obtained for the case of axial flow at the inlet (flow angle of 0°) were as follows:

1. The greatest improvements in the downstream flow distributions in the central region of the duct were obtained with the configurations which had the highest suction flow rates and the most extensive distribution of suction holes downstream from the natural separation region. In order to obtain a uniform flow distribution across the entire duct, boundary-layer control would be required on the outer wall also since suction control caused the outer-wall boundary layer to thicken.

2. For suction flow rates in excess of 1 percent, the measured values of static-pressure rise and total-pressure loss through the diffuser were not affected by the number of rows of suction holes used. With increasing suction flow rate, the measured values of total-pressure loss decreased continuously; whereas, the measured static-pressure rise reached a maximum at a suction flow of 2.8 percent and decreased beyond this point because of the excessive thickening of the outer-wall boundary layer.

3. A suction flow rate of 2.3 percent increased the measured static-pressure rise to stations 0.68 and 1.10 outer diameters downstream from the diffuser inlet by 60 percent and 25 percent, respectively, and decreased the measured total-pressure loss by 63 percent. For one of the best suction-hole configurations, correcting for the suction pumping power reduced the 25-percent increase in static-pressure rise to 22.6 percent and the 63-percent reduction in total-pressure loss to 30 percent.

4. Although the suction pumping power required for the best configurations was not high relative to the increases in performance obtained, the pumping power could have been reduced as much as 40 percent by increasing the total suction hole area. Rounding the edges of the suction holes reduced the pumping power by 30 percent.

Whirling Flow

The results obtained for the case of whirling flow (mean flow angle of 19.5°) at the inlet were as follows:

1. Without straightener vanes the flow distributions downstream from the diffuser were more uniform near the outer wall than with axial flow; however, a reverse-flow region near the duct center line was induced by rotation and intensified by suction control.

2. Although whirl reduced the measured total-pressure losses about 30 percent without suction, the static-pressure rise was low with or without suction because of the high flow angles (mean angle of about 41°) downstream from the diffuser.

3. An attempt to remove the whirl through use of straightener vanes was unsuccessful because a gap between the tip of the vanes and the inner wall allowed appreciable rotation to exist in the region of the inner wall.

Langley Aeronautical Laboratory,
National Advisory Committee for Aeronautics,
Langley Field, Va., September 24, 1956.

REFERENCES

1. Wood, Charles C.: Preliminary Investigation of the Effects of Rectangular Vortex Generators on the Performance of a Short 1.9:1 Straight-Wall Annular Diffuser. NACA RM L51G09, 1951.

2. Wood, Charles C., and Higginbotham, James T.: The Influence of Vortex Generators on the Performance of a Short 1.9:1 Straight-Wall Annular Diffuser With Whirling Inlet Flow. NACA RM L52L01a, 1953.

3. Wood, Charles C., and Higginbotham, James T.: Flow Diffusion in a Constant-Diameter Duct Downstream of an Abruptly Terminated Center Body. NACA RM L53D23, 1953.

4. Wood, Charles C., and Higginbotham, James T.: Performance Characteristics of a 24° Straight-Outer-Wall Annular-Diffuser—Tailpipe Combination Utilizing Rectangular Vortex Generators for Flow Control. NACA RM L53H17a, 1953.

5. Wood, Charles C., and Higginbotham, James T.: Effects of Diffuser and Center-Body Length on Performance of Annular Diffusers With Constant-Diameter Outer Walls and With Vortex-Generator Flow Controls. NACA RM L54G21, 1954.

6. Henry, John R., and Wilbur, Stafford W.: Preliminary Investigation of the Flow in an Annular-Diffuser—Tailpipe Combination With an Abrupt Area Expansion and Suction, Injection, and Vortex-Generator Flow Controls. NACA RM L53K30, 1954.

7. Wilbur, Stafford W., and Higginbotham, James T.: Investigation of Two Short Annular Diffuser Configurations Utilizing Suction and Injection as a Means of Boundary-Layer Control. NACA RM L54K18, 1955.

8. Anon.: Flow Measurement by Means of Standardized Nozzles and Orifice Plates. Supplement on Instruments and Apparatus, pt. 5, ch. 4, Power Test Codes, A.S.M.E., 1949, pp. 5-62.

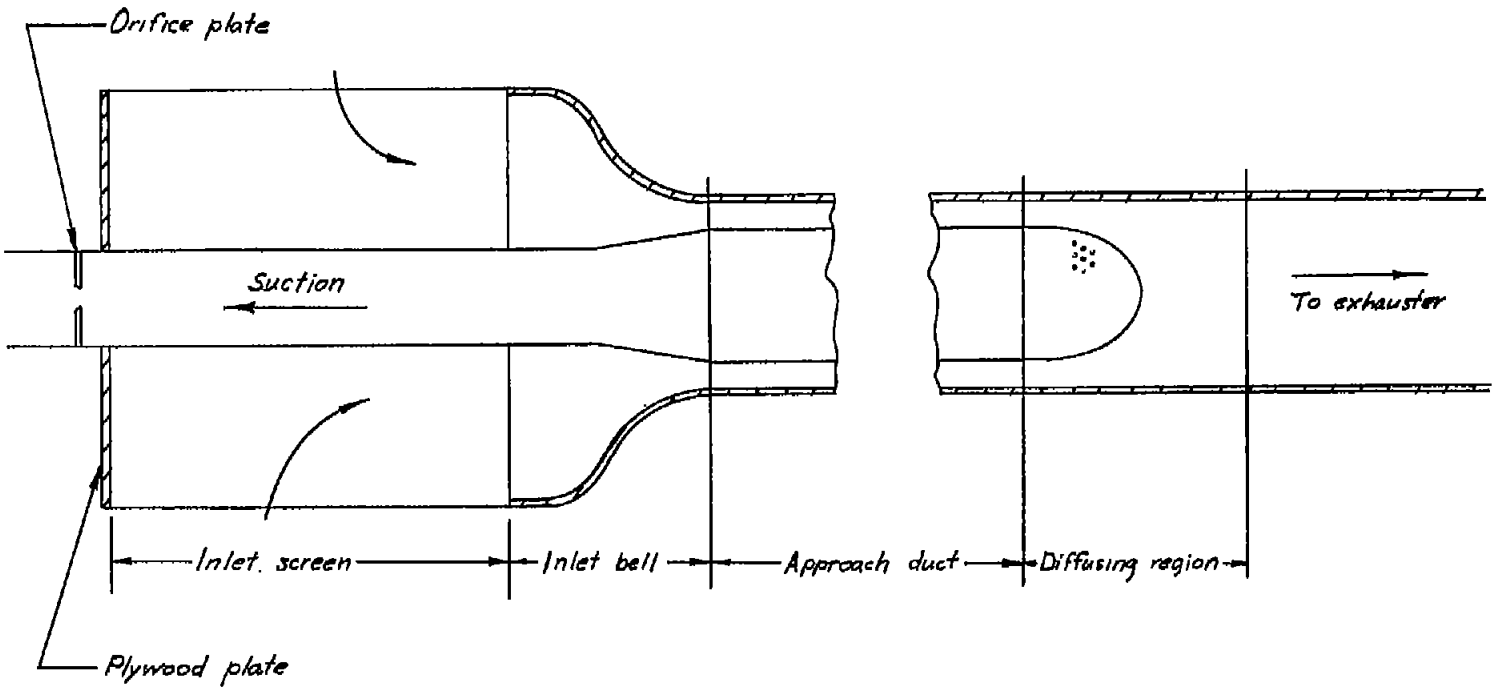

(a) General duct arrangement.

Figure 1.- Test apparatus.

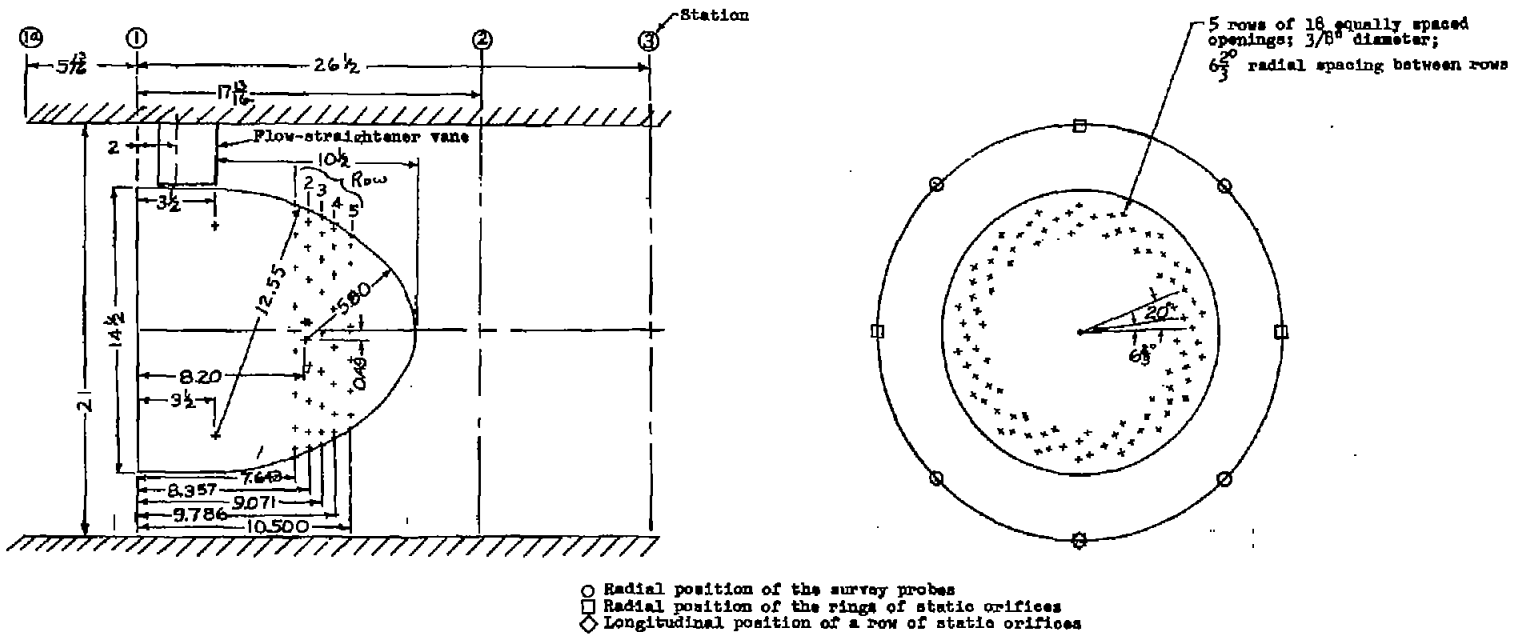

(b) Line drawing of diffuser. All dimensions are in inches unless otherwise indicated.

Figure 1.- Continued

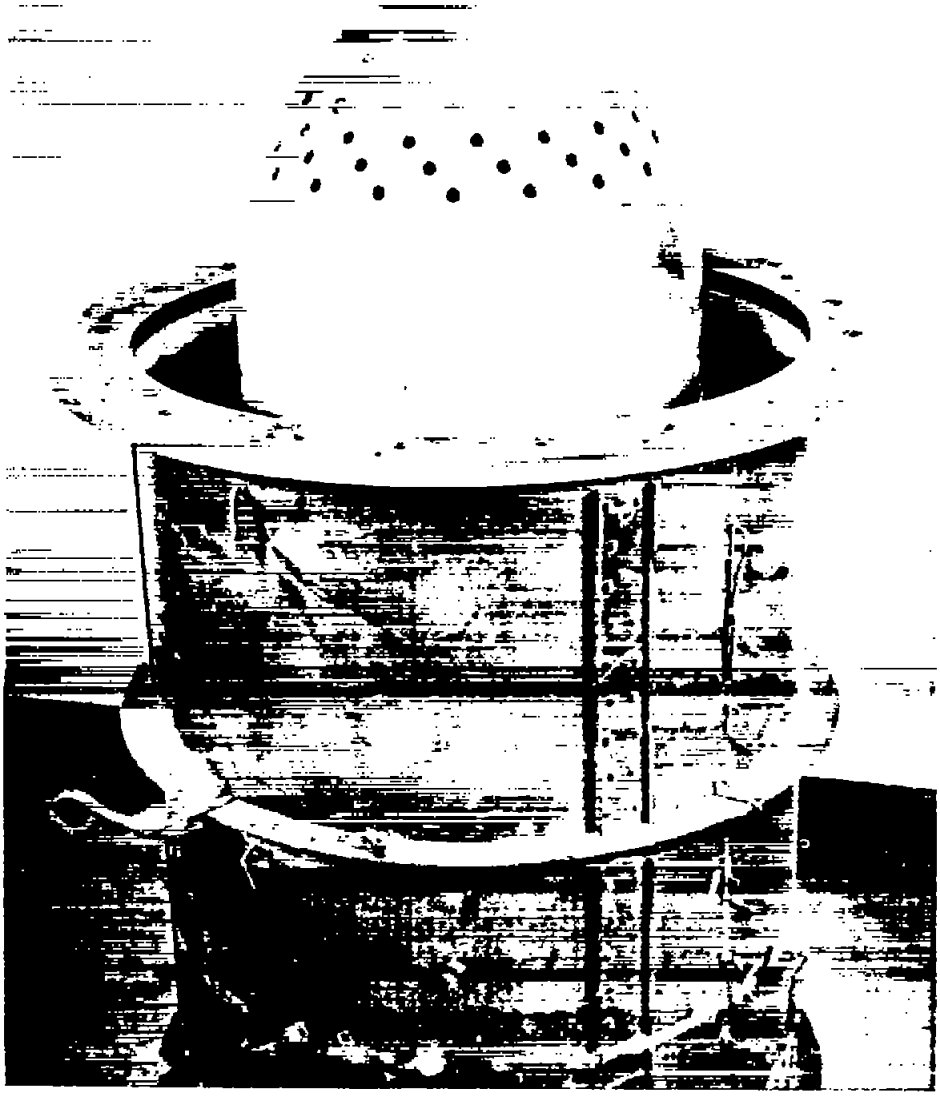

L-94772

(c) Photograph of diffuser.

Figure 1.- Concluded.

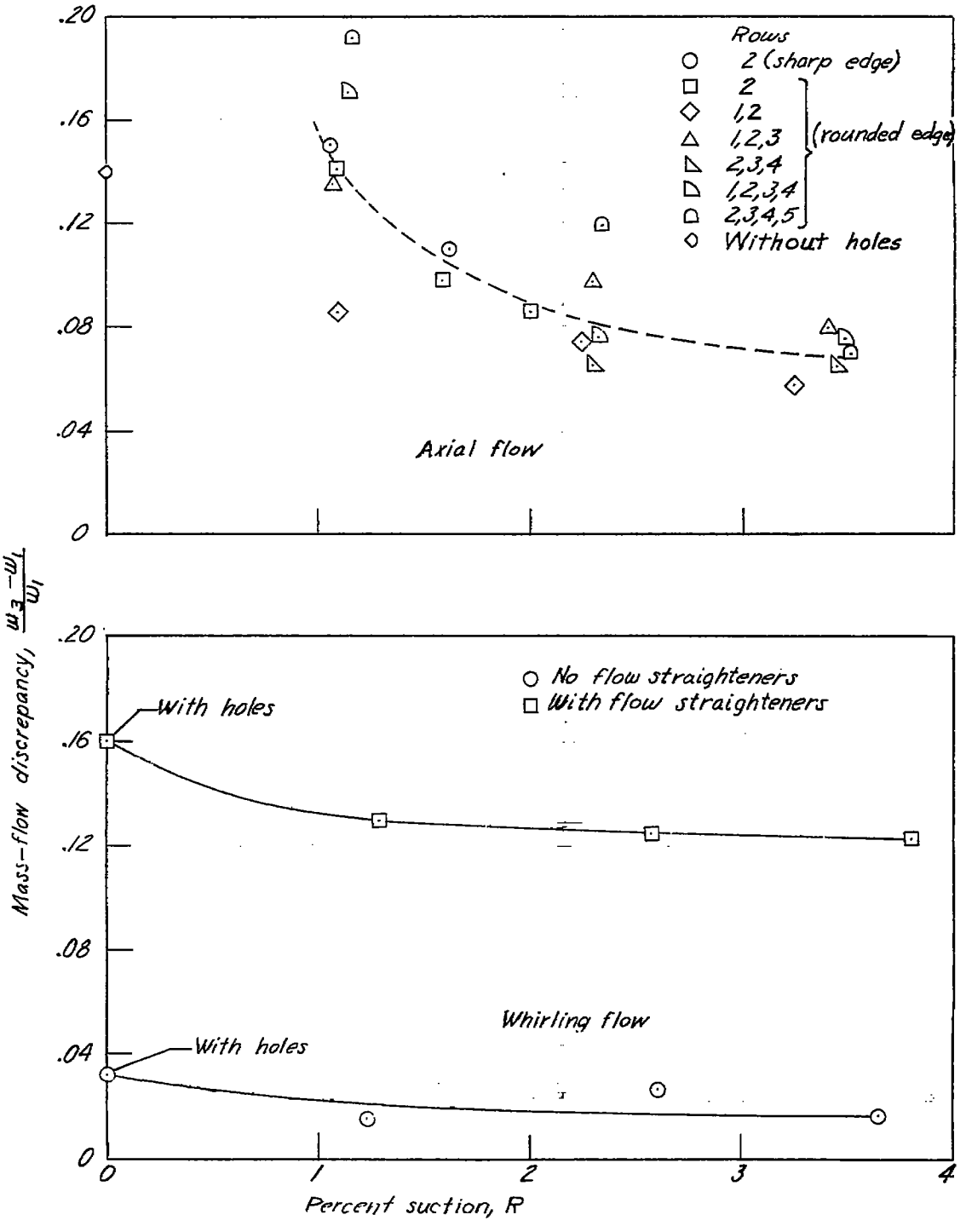

Figure 2.- Variation of the discrepancy between inlet and exit mass-flow measurements with percent suction.

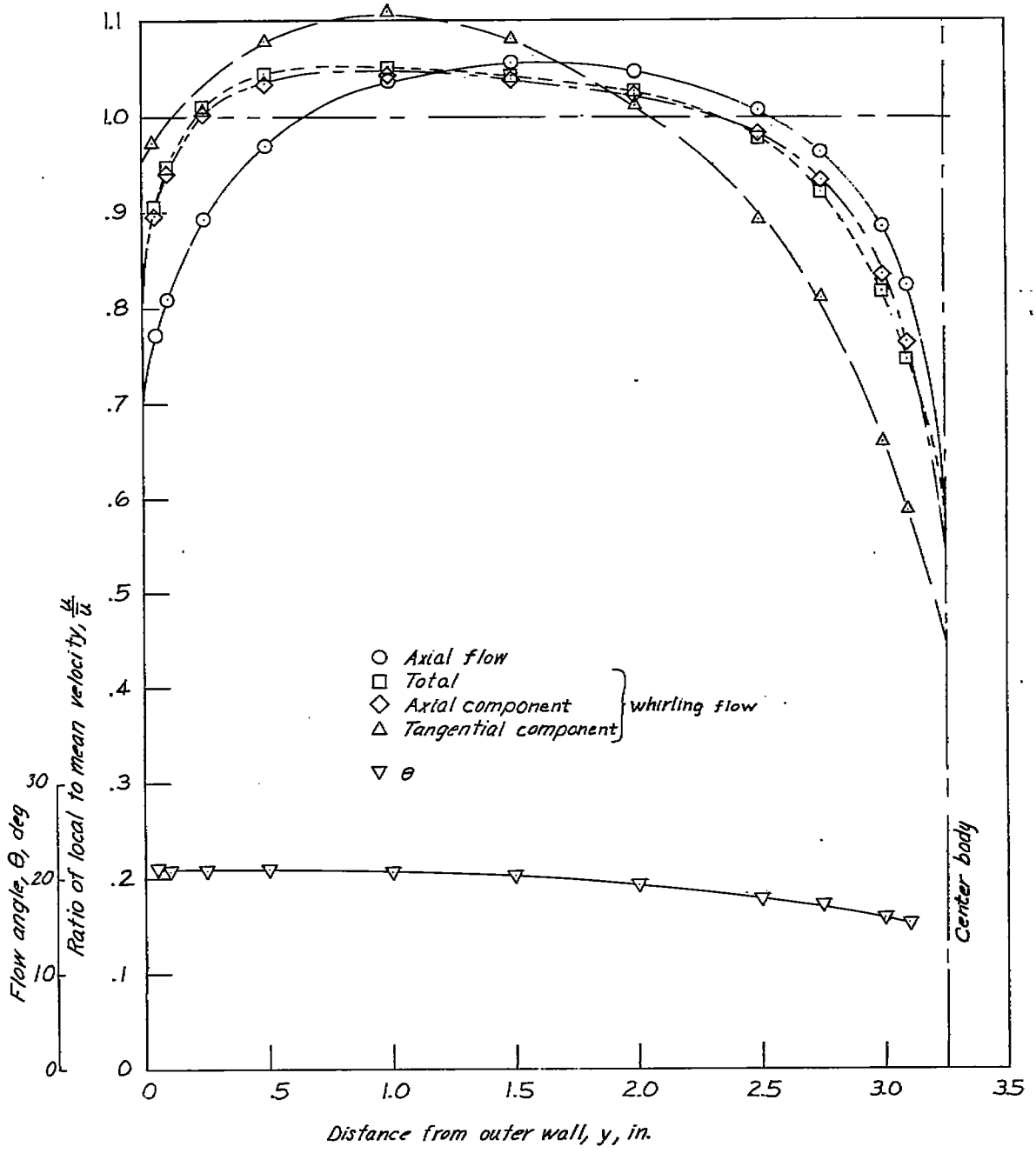

Figure 3.- Inlet velocity and flow-angle distributions.

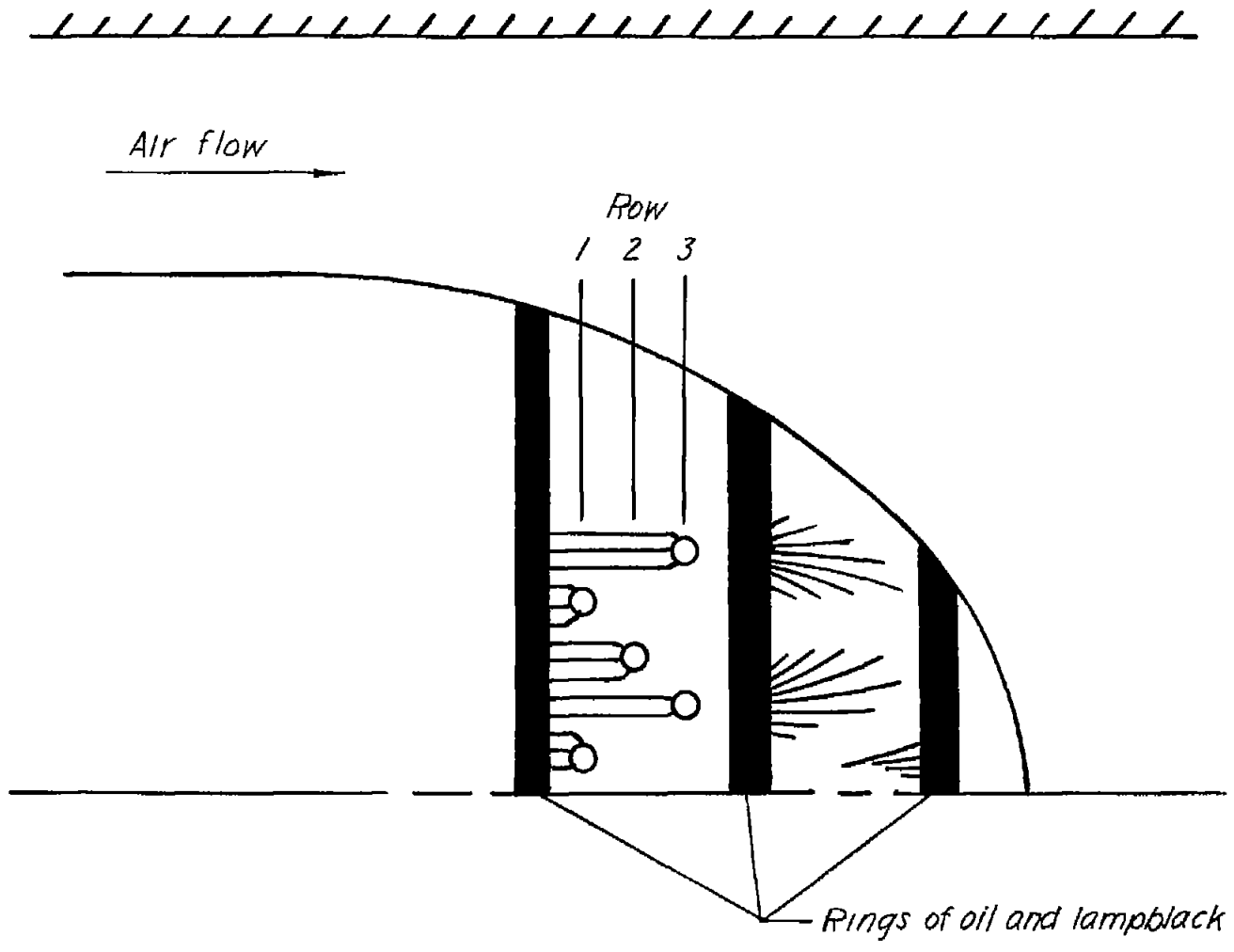

Figure 4.- Visual-flow observations. $\overline{\theta}_1 = 0^\circ$.

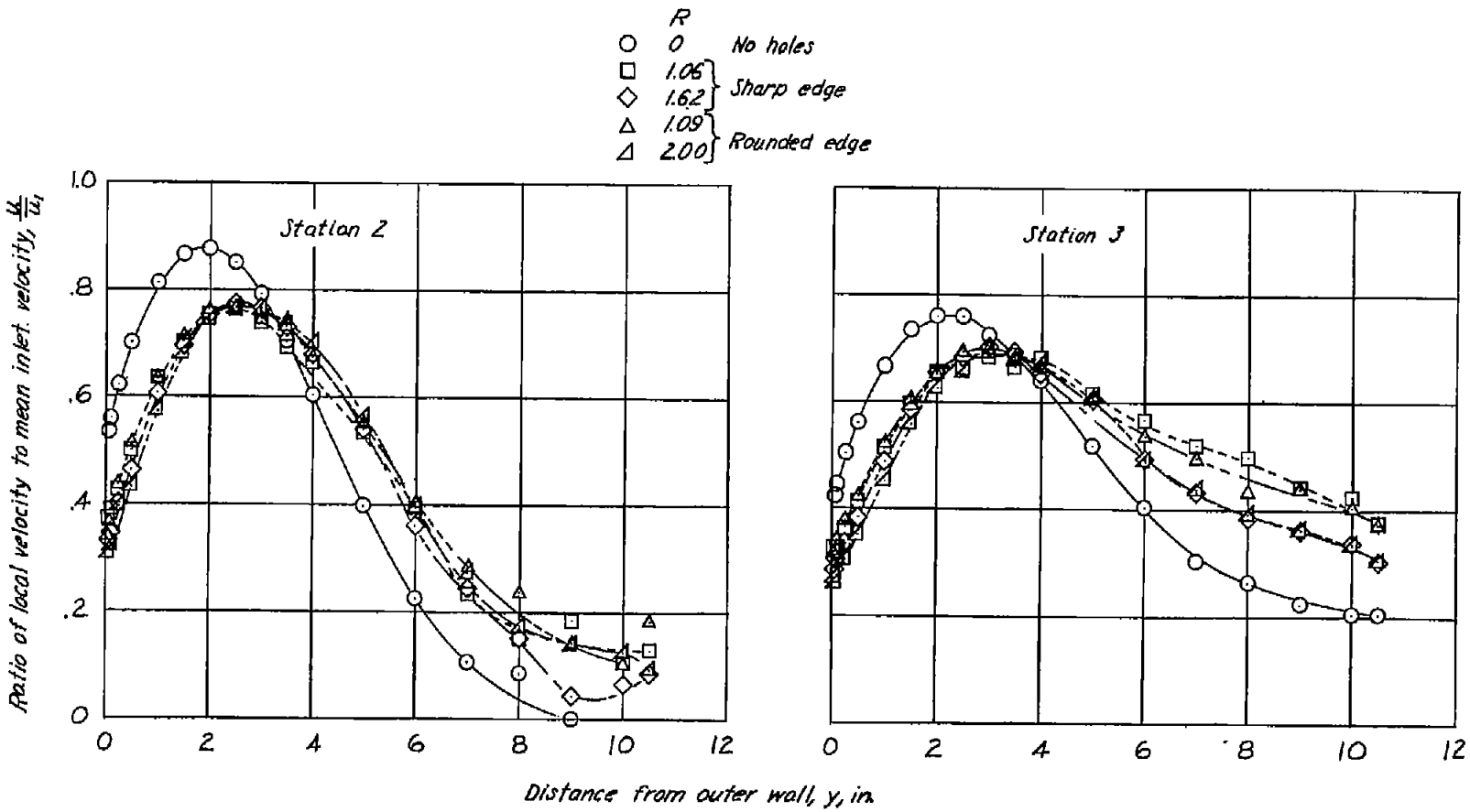

Figure 5.- Velocity distributions at stations 2 and 3 with suction through row 2. $\overline{\theta}_1 = 0^\circ$.

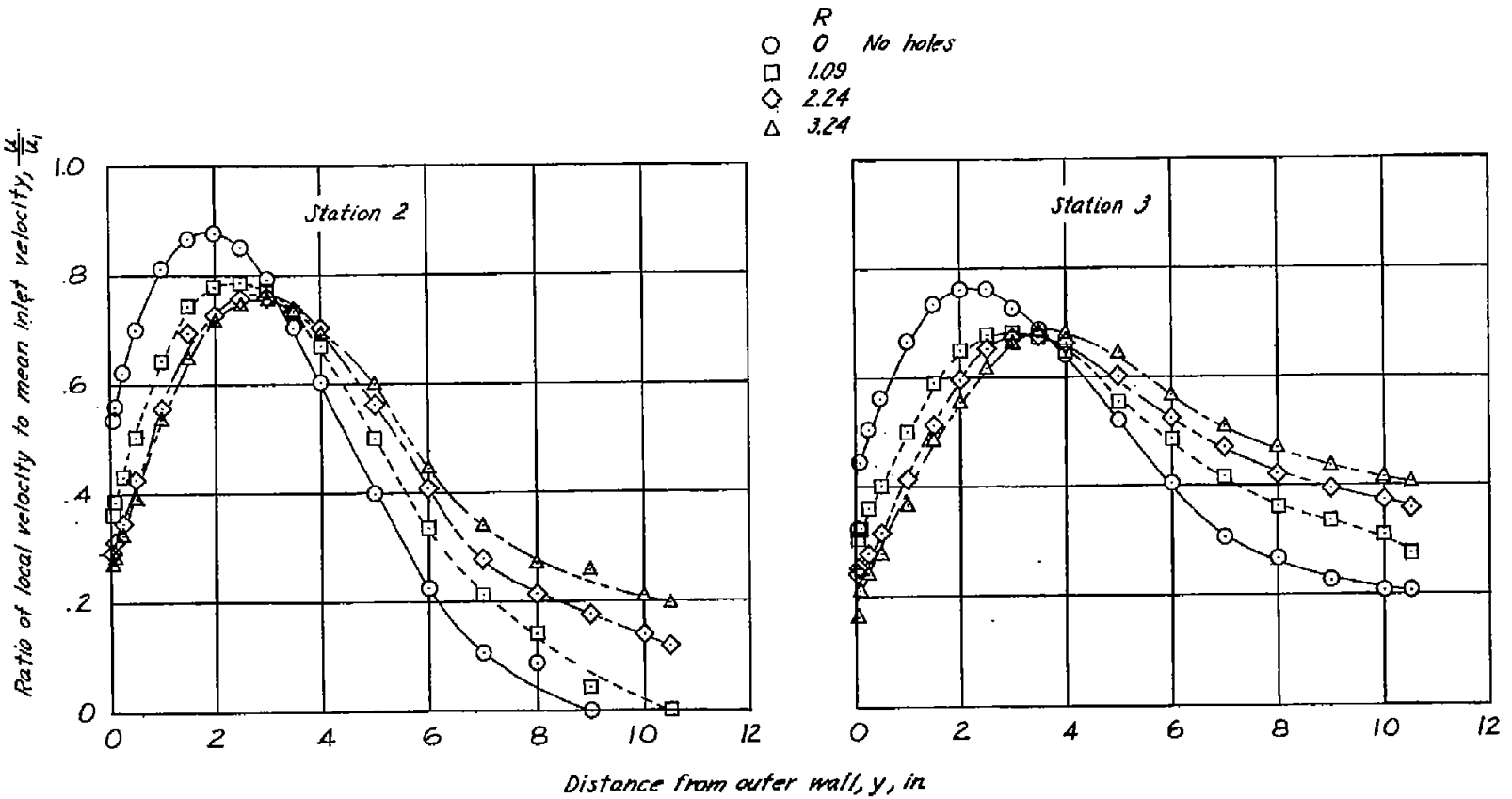

Figure 6.- Velocity distributions at stations 2 and 3 with suction through rows 1 and 2. $\overline{\theta}_1 = 0^\circ$.

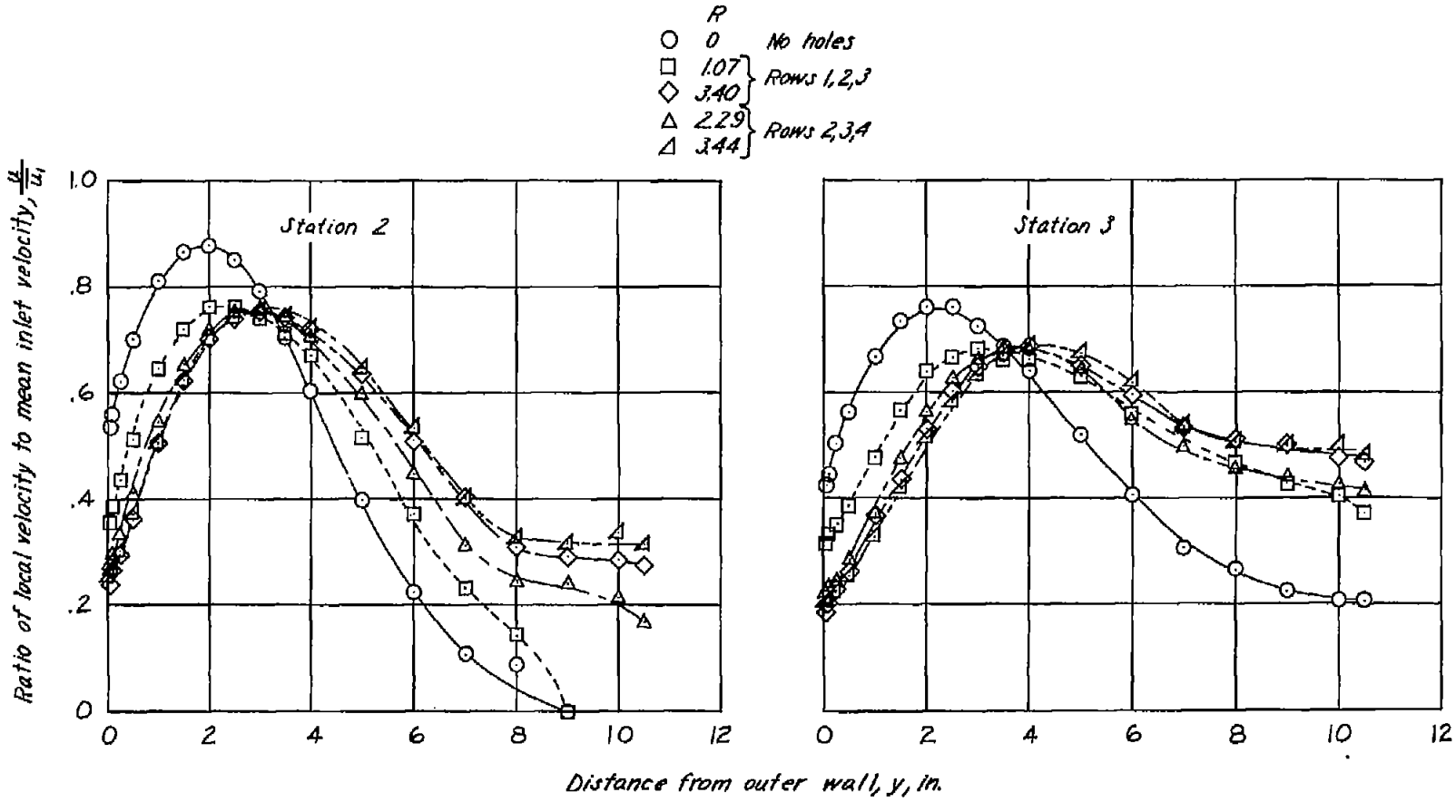

Figure 7.- Velocity distributions at stations 2 and 3 with suction through rows 1, 2, and 3 and 2, 3, and 4. $\overline{\theta}_1 = 0^\circ$.

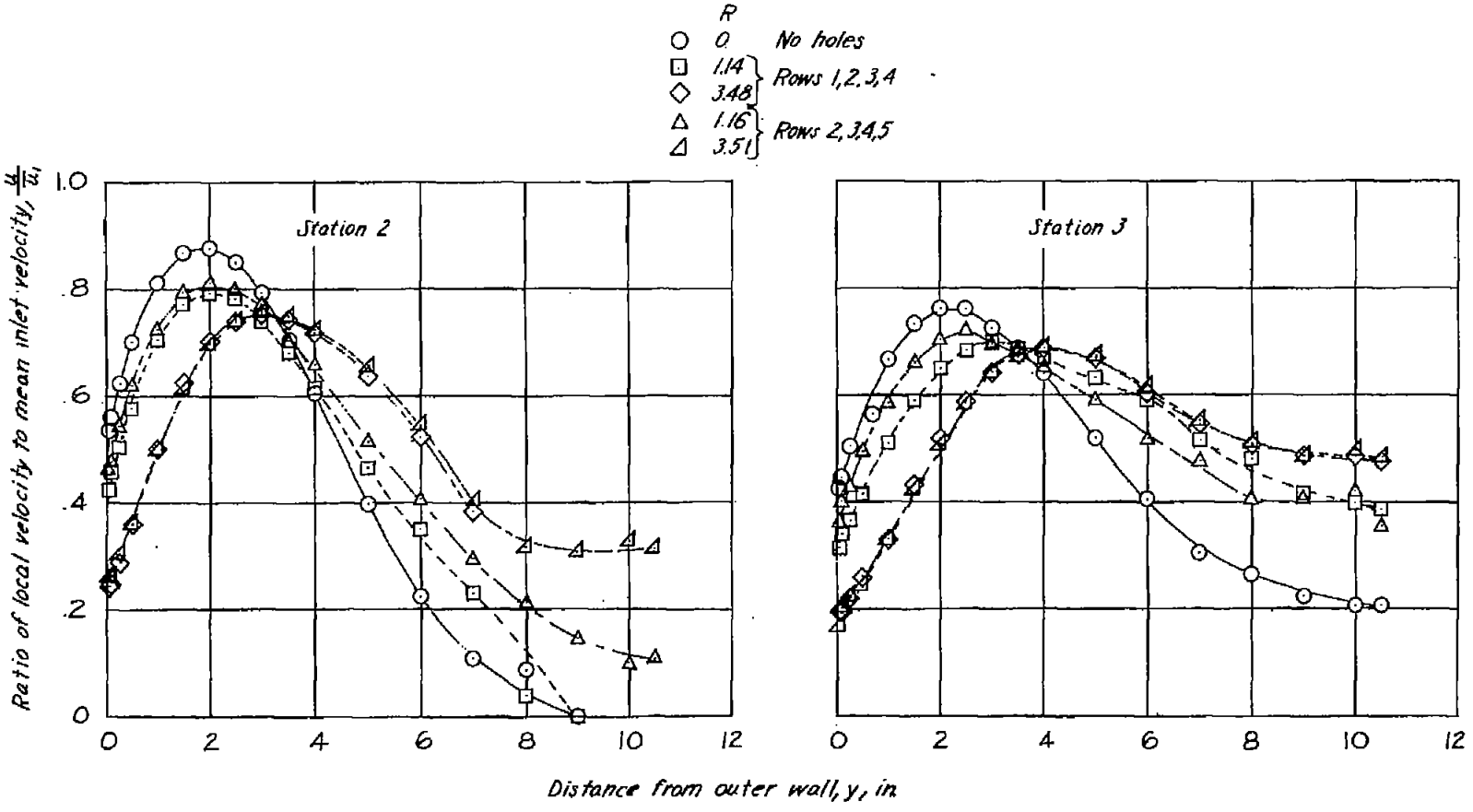

Figure 8.- Velocity distributions at stations 2 and 3 with suction through rows 1, 2, 3, and 4 and 2, 3, 4, and 5. $\overline{\theta}_1 = 0^\circ$.

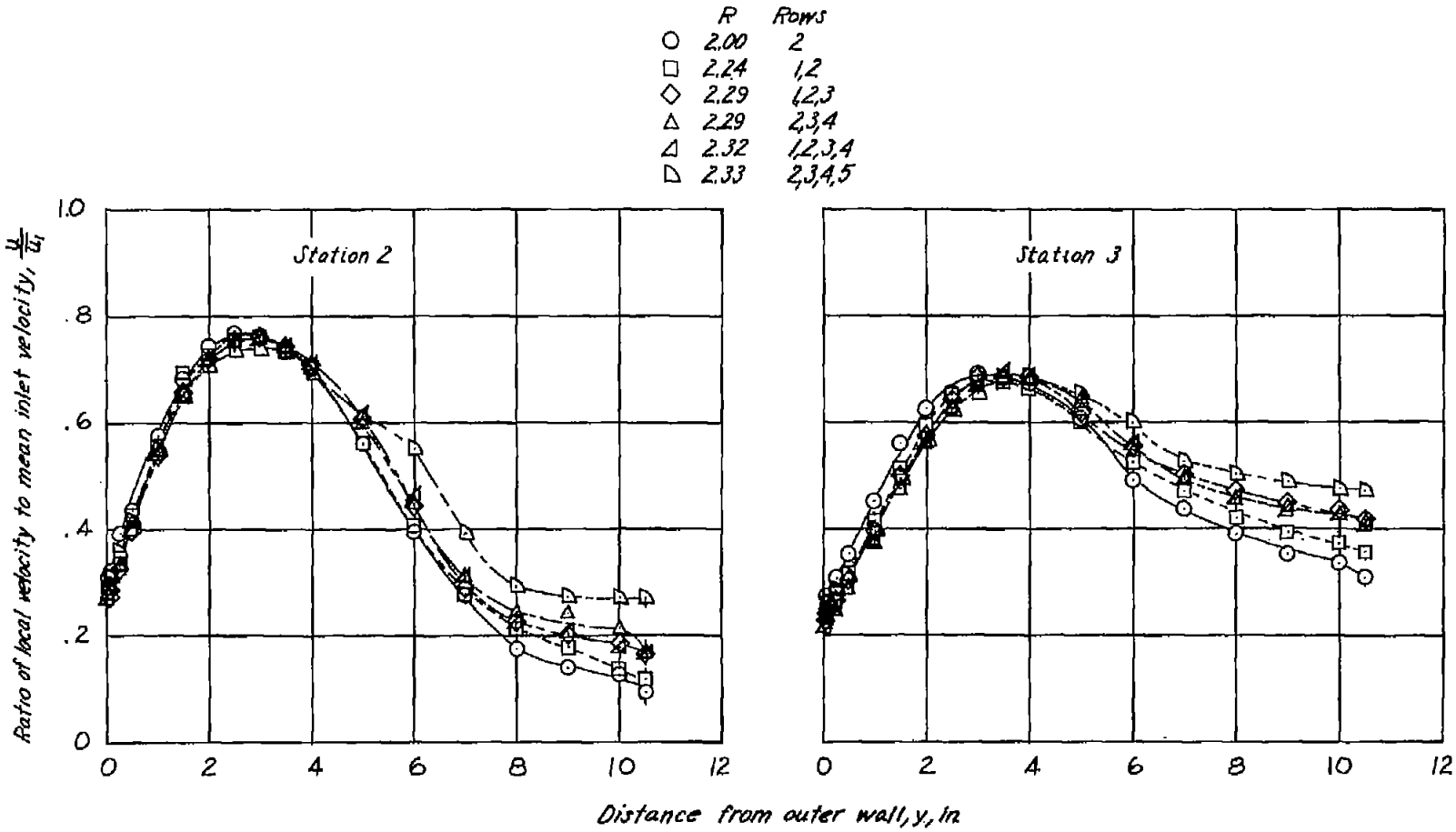

(a) R ≈ 2.3 percent.

Figure 9.- Velocity distributions at stations 2 and 3 with constant suction through various hole combinations. $\overline{\theta}_1 = 0^\circ$.

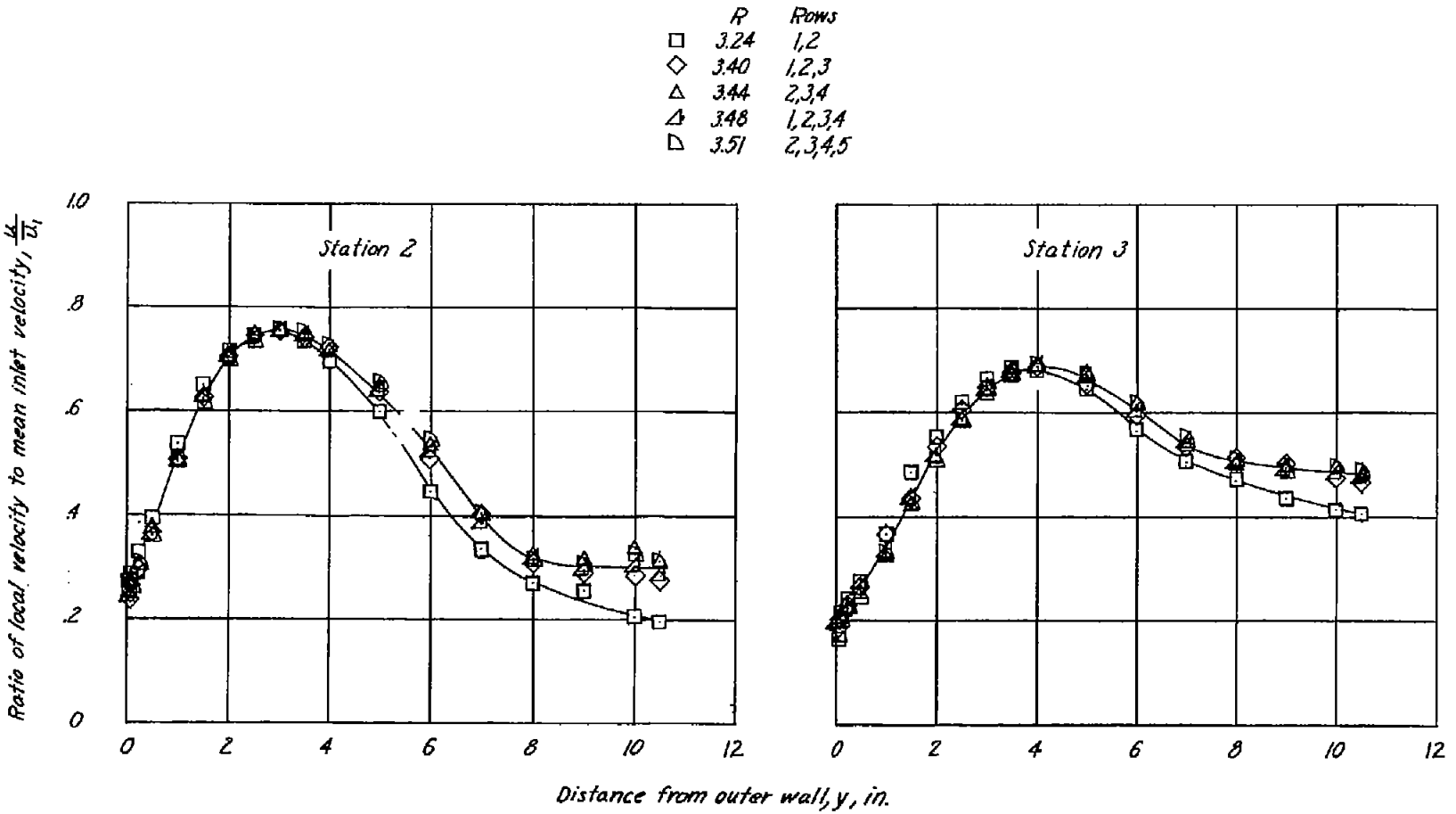

(b) R ≈ 3.4 percent.

Figure 9.- Concluded.

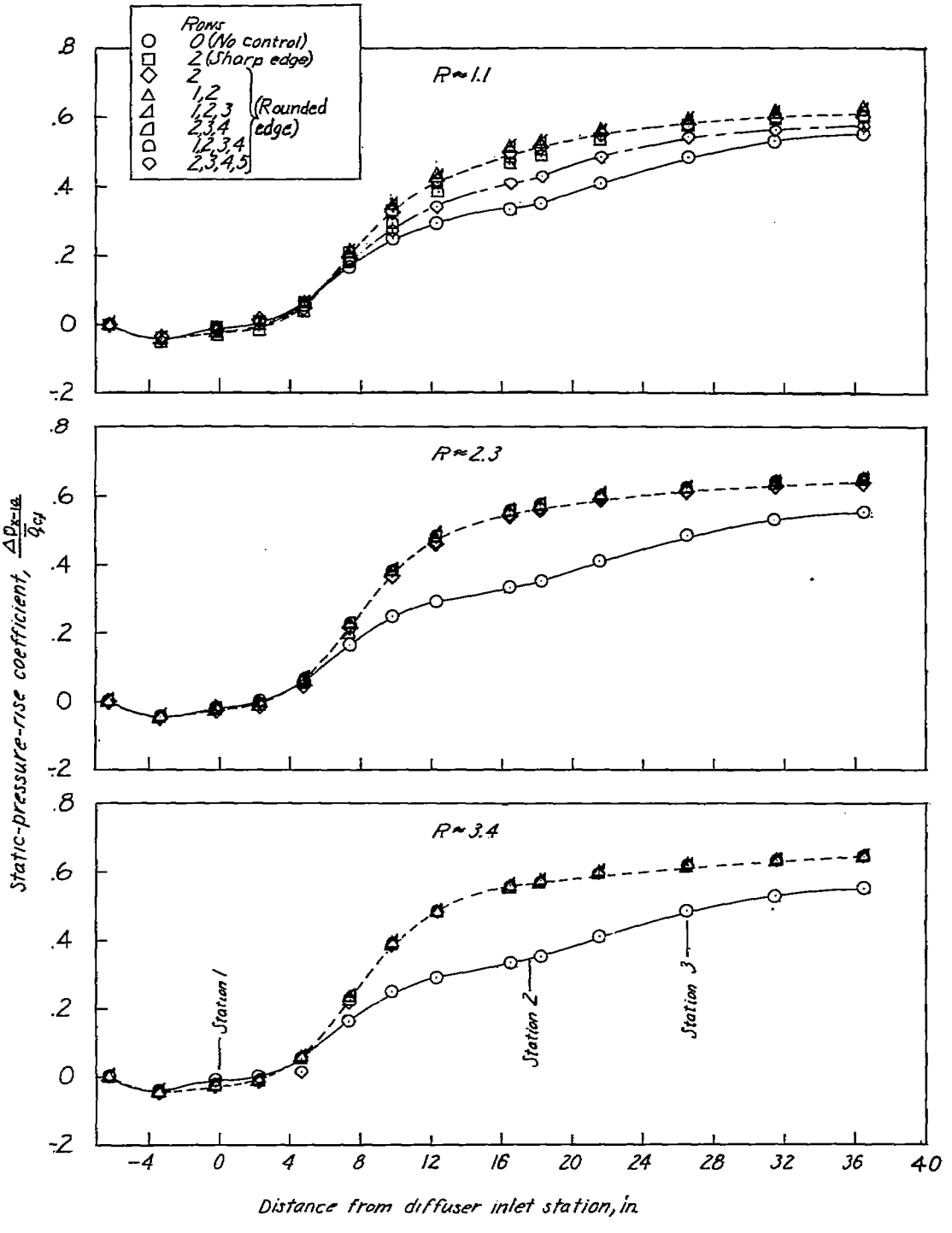

Figure 10.- Static-pressure-rise coefficient along the diffuser outer wall. $\overline{\theta}_1 = 0^\circ$.

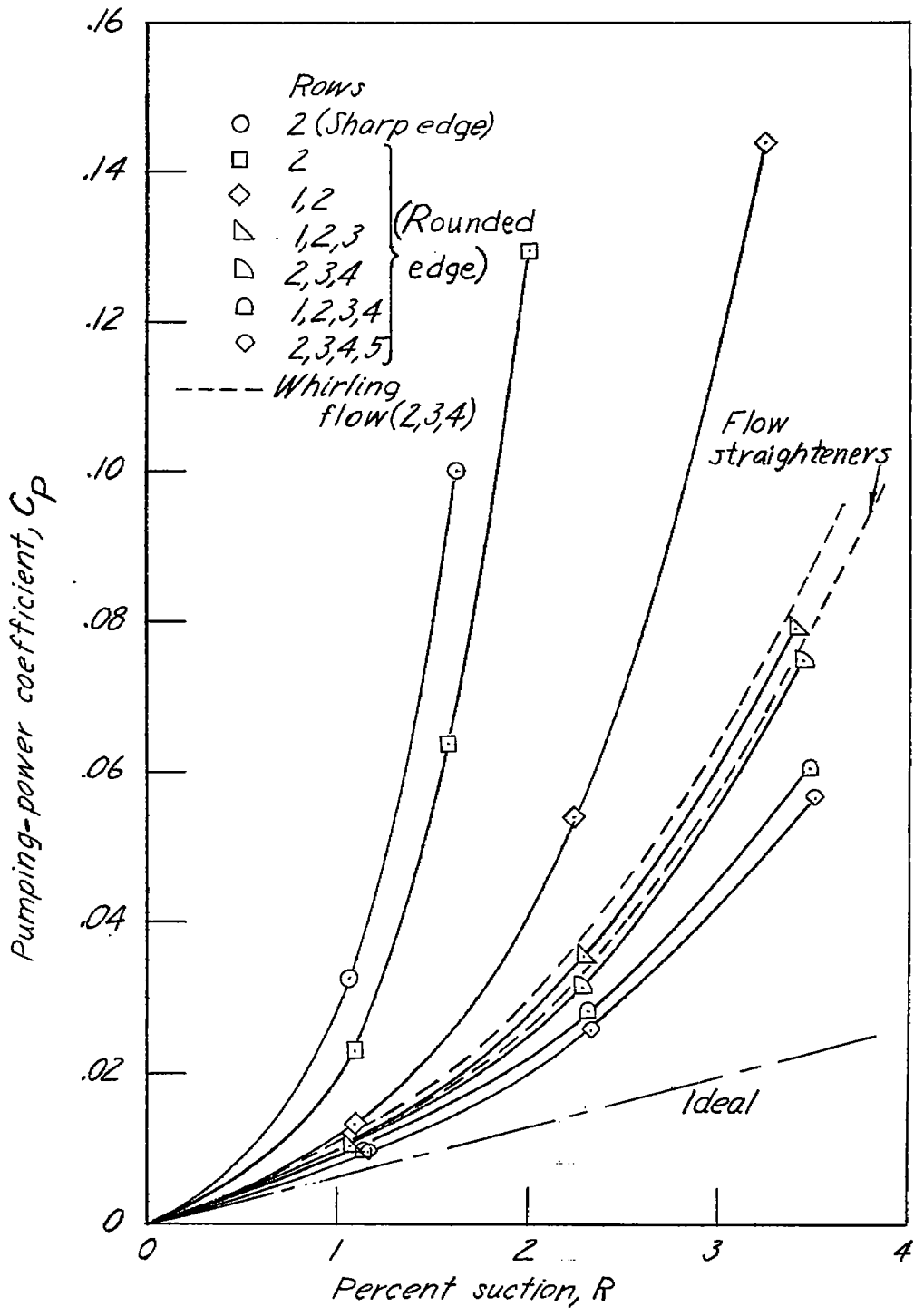

Figure 11.- Variation of pumping-power coefficient with percent suction.

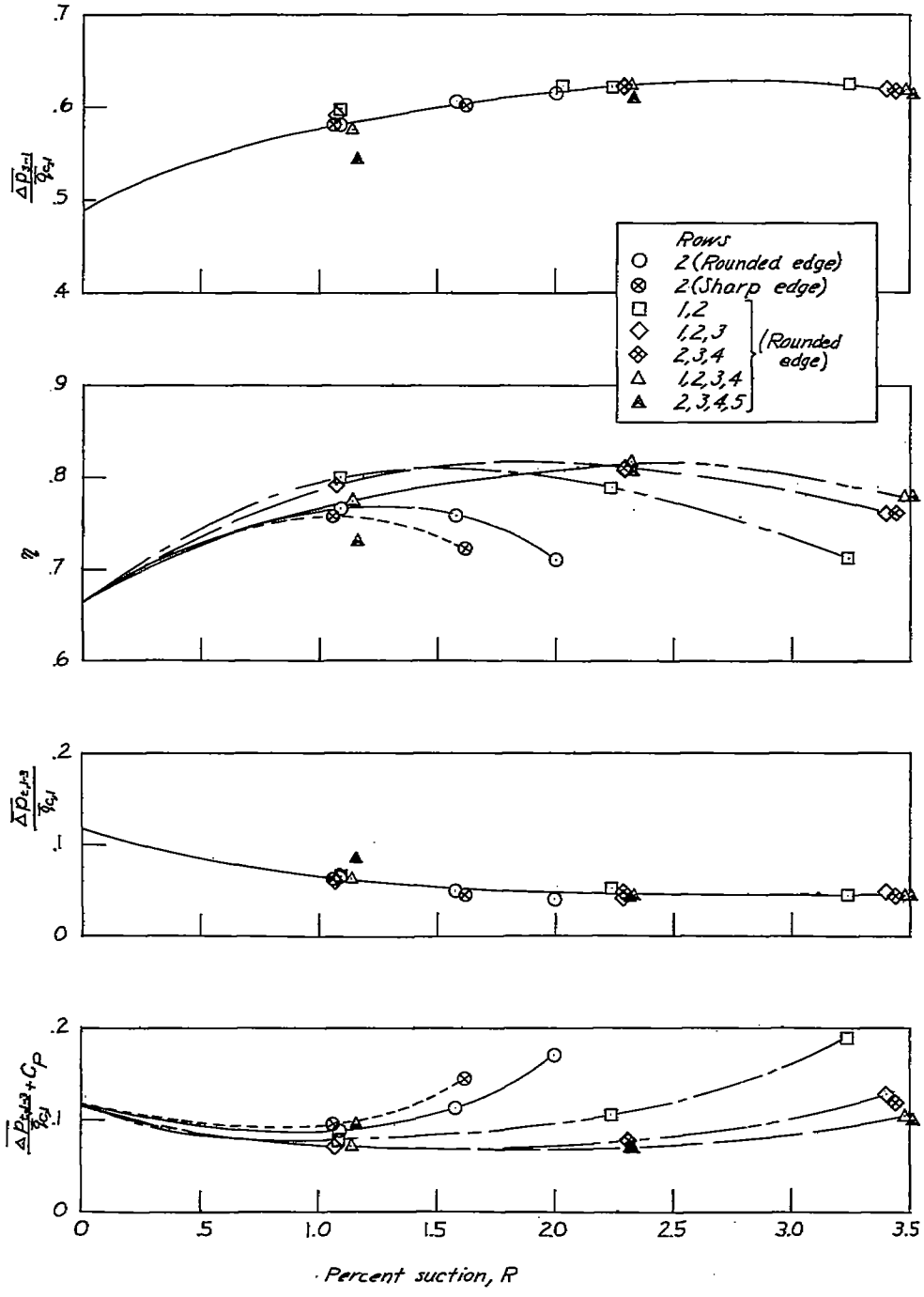

Figure 12.- Variation of static-pressure-rise coefficient, diffuser effectiveness, and loss coefficient at station 3 with percent suction. $\bar{\theta}_1 = 0^\circ$.

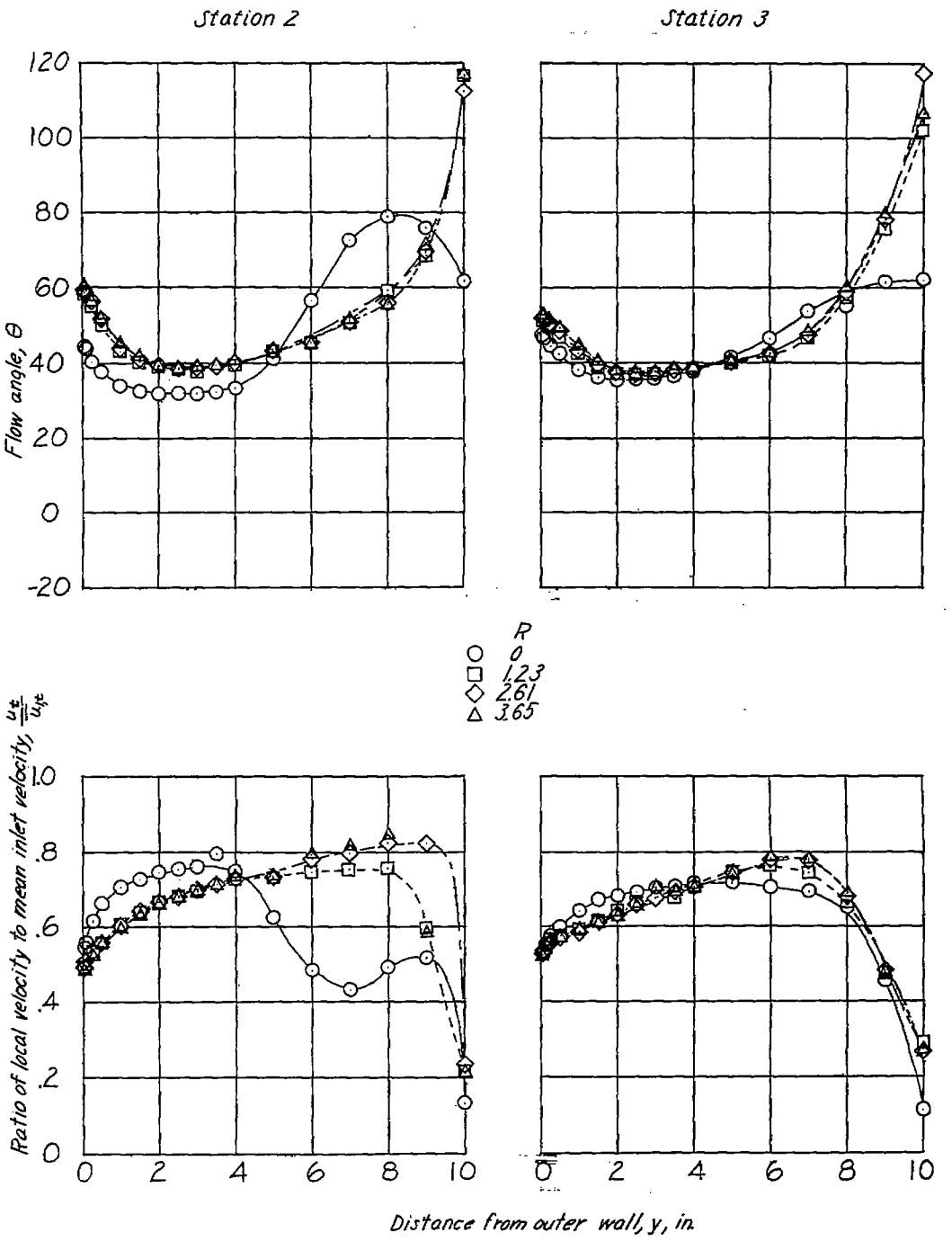

Figure 13.- Velocity and flow-angle distributions at stations 2 and 3 with $\bar{\theta}_1 = 19.5^\circ$ and suction through rows 2, 3, and 4. No flow straighteners.

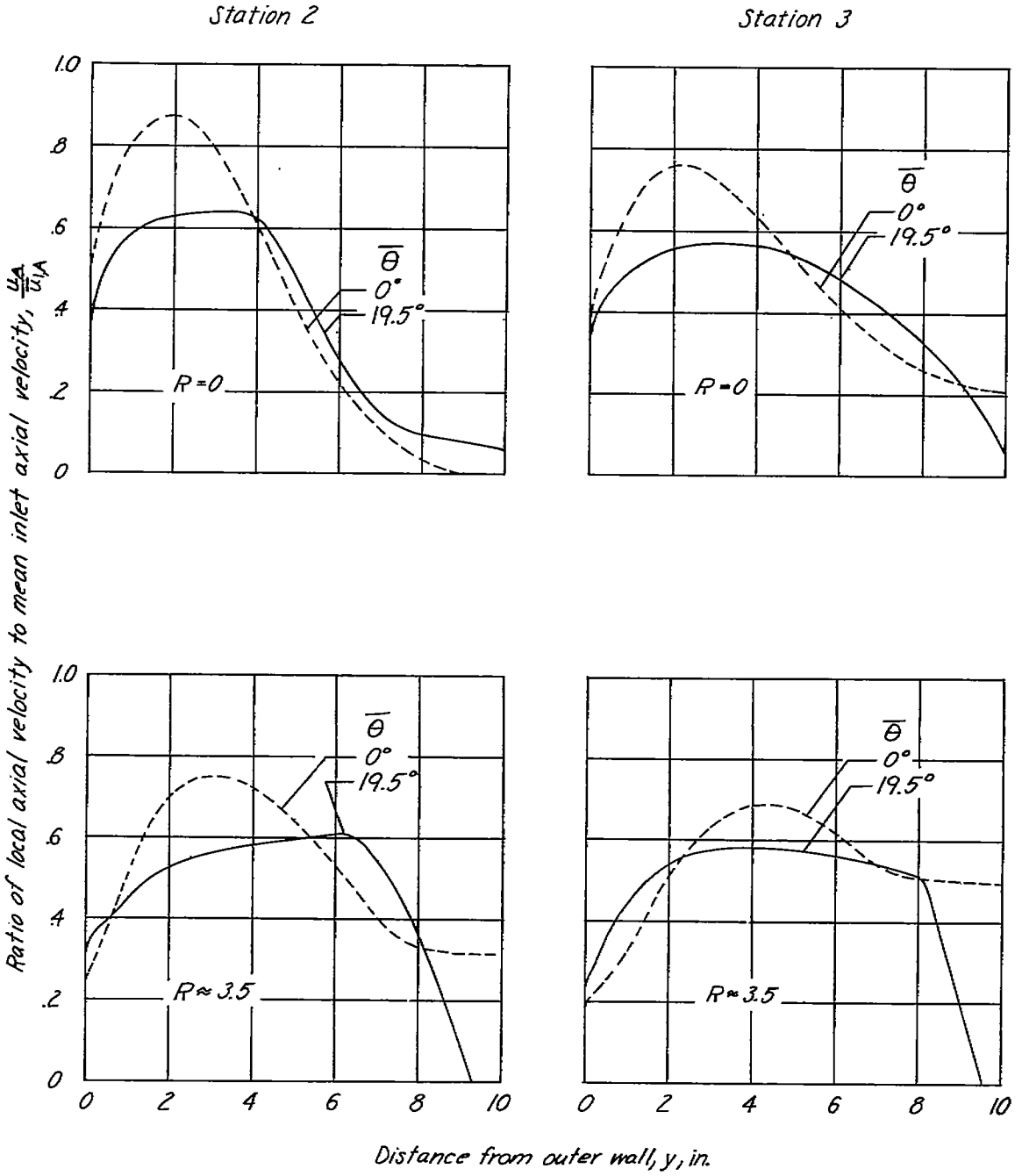

Figure 14.- Comparison of axial-velocity components for $\overline{\theta}_1 = 0°$ and $\overline{\theta}_1 = 19.5°$ at stations 2 and 3. No flow straighteners.

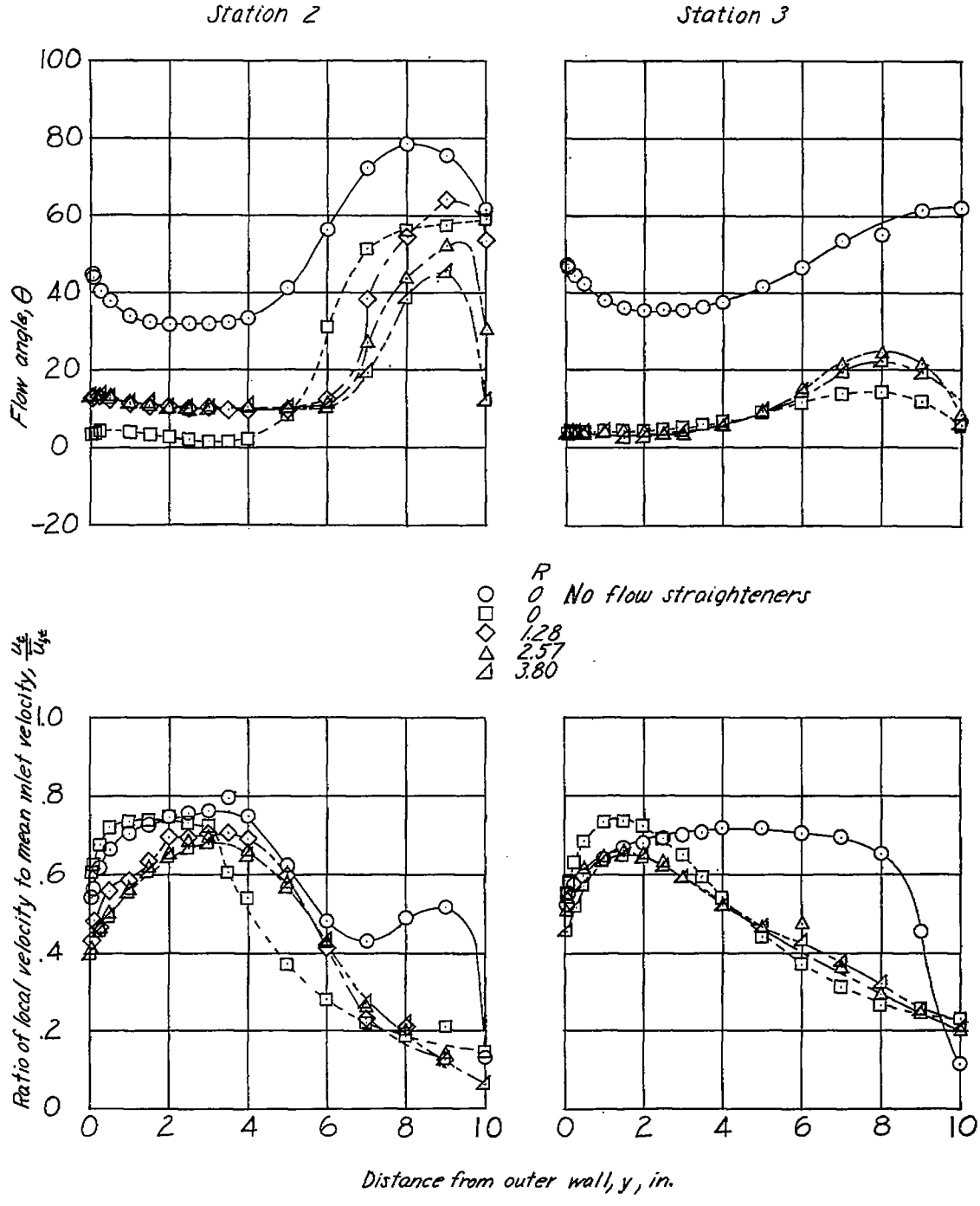

Figure 15.- Velocity and flow-angle distributions at stations 2 and 3 with $\bar{\theta}_1 = 19.5^\circ$ and suction through rows 2, 3, and 4. With flow straighteners.

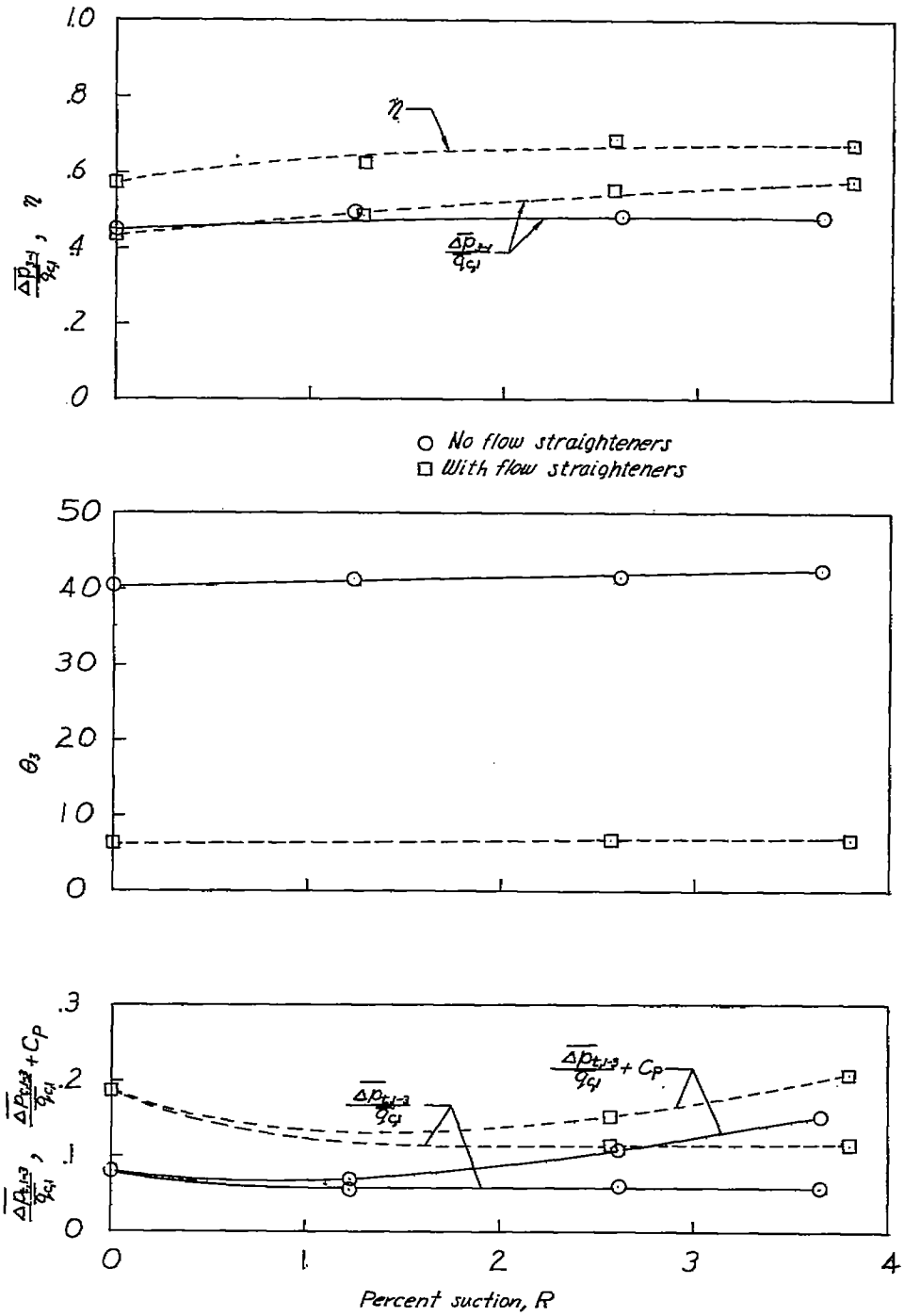

Figure 16.- Variation of static-pressure-rise coefficient, diffuser effectiveness, mean flow angle, and loss coefficient at station 3 with percent suction. $\bar{\theta}_1 = 19.5°$.